

# Panoptic Vision-Language Feature Fields

Haoran Chen<sup>1\*</sup>, Kenneth Blomqvist<sup>1</sup>, Francesco Milano<sup>1</sup> and Roland Siegwart<sup>1</sup>

<sup>1</sup>Autonomous Systems Lab  
ETH Zürich, Zürich, Switzerland  
\*chenhao@student.ethz.ch

**Abstract**—Recently, methods have been proposed for 3D open-vocabulary semantic segmentation. Such methods are able to segment scenes into arbitrary classes given at run-time using their text description. In this paper, we propose to our knowledge the first algorithm for open-vocabulary panoptic segmentation, simultaneously performing both semantic and instance segmentation. Our algorithm, Panoptic Vision-Language Feature Fields (PVLFF) learns a feature field of the scene, jointly learning vision-language features and hierarchical instance features through a contrastive loss function from 2D instance segment proposals on input frames. Our method achieves comparable performance against the state-of-the-art *close-set* 3D panoptic systems on the HyperSim, ScanNet and Replica dataset and outperforms current 3D open-vocabulary systems in terms of semantic segmentation. We additionally ablate our method to demonstrate the effectiveness of our model architecture. Our code will be available at <https://github.com/ethz-asl/autolabel>.

**Index Terms**—3D panoptic segmentation, open vocabulary, neural implicit representation.

## I. INTRODUCTION

An important consideration for building spatial AI applications is the representation used to model the scene. Ideally, the chosen representation can be built incrementally in real-time, models the geometry with high fidelity, and allows for flexible semantic queries to be run against the representation at run-time.

Recently, open-vocabulary semantic scene representations based on NeRF [1] have been proposed [2]–[4] for robotics and spatial AI applications. Such systems reconstruct scene geometry implicitly from 2D views, and enable zero-shot semantic segmentation and natural language-based object detection, without knowing what the query classes or prompts will be at training time. They achieve this by distilling features from a vision-language model into a feature field representation mapping points in the scene to vision-language vectors, which can be compared against natural language prompts. Such representations present great promise for augmented reality, mobile manipulation and intelligent robotics applications, where they open up the possibility of bridging physical 3D spaces with natural language representations.

A limitation of current systems is that while they are able to tell different classes apart, they are unable to tell instances of objects belonging to the same class apart. That is, they are able to perform *semantic* segmentation, but cannot produce a *panoptic* segmentation of the scene. A key problem in 3D instance segmentations that are built from multiple views is that instance segmentations across individual views are not guaranteed to be consistent. This is further complicated by

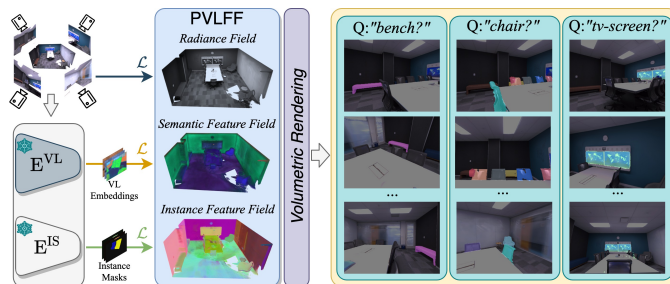


Fig. 1. **Overview of PVLFF.** Given 2D posed images, PVLFF optimizes a semantic feature field by distilling vision-language embeddings from off-the-shelf network  $E_{VL}$ , and simultaneously trains an instance feature field through contrastive learning based on 2D instance proposals computed by  $E_{IS}$ . After training through different loss functions ( $\mathcal{L}$ ), PVLFF is able to perform panoptic segmentation under open-vocabulary prompts.

the fact that 2D segments are noisy, and might only segment a subpart of each object in individual views.

A recent approach, Panoptic Lifting [5], tackles panoptic segmentation by fusing 2D panoptic segmentations into 3D by mapping instance identifiers in different views through a linear assignment. A drawback of this approach is that it assumes a maximum number of instances in the scene, and requires computing the assignment at each training step, which is increasingly expensive as the assumed number of instances grows. Furthermore, the semantic predictions of Panoptic Lifting are restricted to a fixed set of semantic categories.

In this work, we propose Panoptic Vision-Language Feature Fields (PVLFF), a novel pipeline for 3D open-vocabulary panoptic mapping. Our core insight is that existing vision-language feature field approaches [2]–[4] can be extended to do panoptic segmentation by introducing a separate instance feature head, which is learned from 2D instance segment proposals using a contrastive loss function. The contrastive loss function enables learning from inconsistent instance segments and does not require assuming a maximum instance count. At run time, instance features can be easily clustered using conventional hierarchical clustering methods to produce an instance segmentation, either of the 3D representation or of rendered 2D views of the scene. The resulting instance segments can be fused with the semantic segmentation to produce a panoptic segmentation. We furthermore show that the learned instance features follow a hierarchical structure, which enables instances to be segmented at different scales.

We evaluate PVLFF on the Hypersim [6], Replica [7] and ScanNet [8] datasets. Our method achieves comparable results

against state-of-the-art *close-set* panoptic systems. We also show that our method outperforms zero-shot methods on both 2D and 3D semantic segmentation (+4.6% of mIoU). We further ablate the design choices of our method.

In summary, our contributions are:

- A hierarchical instance feature field that enables obtaining 3D instance segments from 2D proposals using contrastive learning;
- To the best of our knowledge, the first zero-shot open-vocabulary panoptic segmentation system.

## II. RELATED WORK

**Panoptic Segmentation.** The task of (2D) panoptic segmentation was first introduced by Kirillov *et al.* [9] to provide a unified vision system that would produce coherent segmentations for both *stuff* – generic amorphous regions, historically the focus of semantic segmentation – and *things* – countable objects, that instance segmentation works aim to delineate. Specifically, the goal of panoptic segmentation is to assign a semantic label and an instance label to each pixel in an image [9]. After a first wave of works [9]–[11] in 2D panoptic segmentation, numerous works have explored panoptic segmentation in a 3D context. [12]–[14] take 3D structures (*e.g.*, point cloud, mesh) as input to predict 3D panoptic segmentation. [15]–[17] propose to simultaneously segment a 3D scene and reconstruct the geometry from 2D images. Recently, NeRF-based methods [5], [18]–[20] have achieved state-of-the-art performance on 3D benchmarks. Most of these methods, however, are task-oriented and none of them are capable of panoptic segmentation in an open set. In this work, we extend NeRF-based methods and propose a 3D panoptic system for open-vocabulary scene understanding.

**Semantic Neural Fields.** Neural fields have become an established representation for 3D scene reconstruction from 2D images ever since the introduction of NeRF [1], which aims to model density and radiance for any 3D position in the scene. NeRF-based systems [21]–[23] have shown impressive results in photo-realistic rendering from novel viewpoints and accurate reconstruction of the scene geometry. Exploiting its 3D-aware nature, recent works have explored extensions of NeRF to high-level tasks, such as fusing semantic information into 3D for scene-level semantic understanding, by using additional neural fields [24], [25]. A limitation of these methods is that they rely on 2D semantic supervision, provided in the form of labels from a fixed, *closed* set. Our method, in contrast, performs semantic segmentation under open-vocabulary queries, while additionally acquiring instance-aware scene knowledge.

**Open-vocabulary Scene Understanding.** In the last few years, several advances in open-vocabulary perception tasks have been achieved by leveraging CLIP [26], a neural network that embeds visual and language information in the same feature space using contrastive learning. In particular, [27]–[29] extended CLIP to pixel-level semantic segmentation by generating a set of class-agnostic dense masks with corresponding class embeddings and selecting during inference the mask with embedding closest to the language query

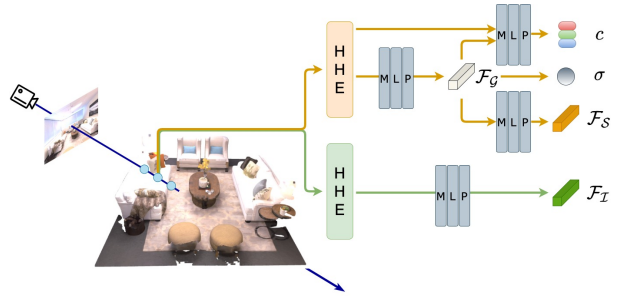


Fig. 2. **Architecture of PVLFF.** Given a 3D coordinate  $\mathbf{x}$  and a unit direction  $\mathbf{d}_r$ , PVLFF uses two sets of hybrid hash encoding (HHE) to parameterize the 3D volume for panoptic scene understanding. With one HHE, we encode color  $c$ , density  $\sigma$  and semantic feature  $\mathcal{F}_S$ . With the other HHE, we exclusively learn instance feature  $\mathcal{F}_I$ . All these scene properties are modeled by lightweight MLPs.

embedding. [30], [31] follow a similar scheme, but focus on per-pixel embeddings, predicting semantics according to the similarity of each pixel with the language query embedding. While the above methods perform 2D tasks, a number of subsequent works have proposed fusing open-vocabulary information into a 3D representation [2]–[4], [32]–[34]. [32], [33] perform open-vocabulary semantic segmentation on pre-computed 3D data structures. [2]–[4], on the other hand, distill the open-vocabulary knowledge into a 3D representation while is reconstructed concurrently. [34] proposes a robot system with language-conditioned robotic control policies to perform complex tasks under natural language instructions. In our work, we mainly focus on panoptic scene understanding under open-vocabulary language queries by fusing pre-trained vision-language knowledge with instance information derived from our instance feature field.

## III. METHOD

In this Section, we describe our approach, PVLFF, as illustrated in Fig. 2. Given a set of posed images  $\{I\}$  of a scene, our objective is to reconstruct a volumetric, implicit representation that encodes color, density, and 3D instances with associated semantics.

We first use a pre-trained open-vocabulary 2D Vision-Language (VL) network to compute pixel-level semantic features for each image of the scene. We then compute instance masks for every image using a pre-trained 2D instance segmentation network. After these preprocessing steps, we build two separate feature fields to distill the precomputed VL embeddings into semantic features, while simultaneously learning a radiance field of the scene and 3D-consistent instance features through contrastive learning using the precomputed 2D instance masks, as shown in Fig. 3. Finally, we combine the semantic and instance features to perform open-vocabulary panoptic segmentation. Detailed explanations of each part are provided in the following Sections.

### A. Data Preprocessing

**VL embedding extraction.** For every RGB image  $I$ , which is assumed to have resolution  $H \times W$ , we compute correspond-

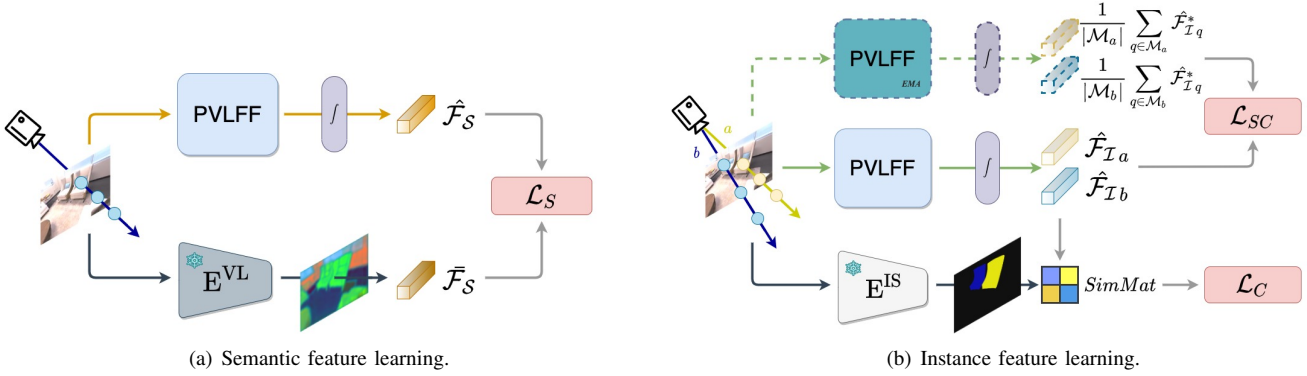


Fig. 3. **PVLFF Optimization.** We optimize the panoptic feature fields by distilling the knowledge from off-the-shelf 2D models. For semantic feature learning 3(a), we compare rendered semantic features with precomputed pixel-level VL embeddings. For instance feature learning 3(b), we pre-compute instance masks using a 2D instance segmenter. We then sample pixels across masks to form positive and negative pairs, and render corresponding instance features. We compute similarity among pairs and optimize instance features by contrastive learning. In addition, we estimate the feature center of each instance mask using instance feature field with EMA parameters and apply a  $l_1$  centralization loss for the instance features.

ing pixel-level embeddings from a frozen VL model  $E^{VL}$ :

$$\bar{\mathcal{F}}_S = E_v^{VL}(I), \quad (1)$$

where  $\bar{\mathcal{F}}_S \in \mathbb{R}^{H \times W \times C}$  denotes the VL embeddings with  $C$  channels upsampled to the same resolution as  $I$ , and  $E_v^{VL}$  denotes the visual encoder in the VL model.

**Instance mask extraction.** In addition to the VL embeddings, we compute instance masks for every image  $I$  using a frozen instance segmenter  $E^{IS}$ :

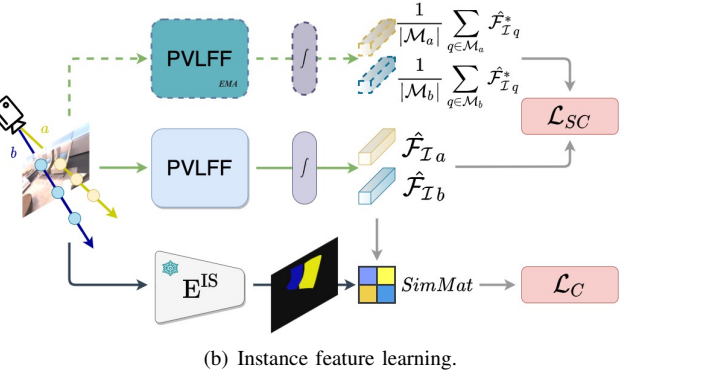
$$[\mathcal{M}]_k = E^{IS}(I), \quad (2)$$

where  $[\mathcal{M}]_k$  denotes a list of binary instance masks generated by  $E^{IS}$  for image  $I$ , and  $k$  denotes the instance identifier. The instance segmenter produces a set of instance segment proposals for each frame. Note that the instance segments do not have to be multi-view consistent and do not have to cover all the pixels. Furthermore, there can be multi-level instance proposals for some pixels. In our experiments, we use the SAM model [35] as the instance segmenter.

## B. Model Structure

Fig. 2 illustrates the structure of our model. We construct a semantic and an instance feature field starting from the NeRF architecture. However, unlike previous methods that stack additional feature fields directly on top of the density and color MLPs (*scene reconstruction* branch) [5], [18], [19], we separate the panoptic feature fields by deriving semantic features  $\mathcal{F}_S$  from the NeRF “geometric” features  $\mathcal{F}_G$  and instance features  $\mathcal{F}_I$  from a separate hybrid hash encoding (HHE) [36].

We experimentally noticed that introducing an instance field helps the quality of VL embeddings derived from the semantic feature field. This observation is validated in ablation experiments in Sec. IV-E. We also found that decoupling the feature fields into different branches benefits the mapping from the underlying HHE to different types of information, and



results in better scene understanding. Moreover, we noticed that geometric features already encode semantic information to some extent from the *color* supervision when learning pure radiance fields. Therefore, we separate the semantic and instance features into two branches. We predict semantic features from scene geometric features, similar to [3], and simultaneously optimize instance features in another branch.

Thus, we formulate panoptic feature fields as follows:

$$\mathcal{F}_I := \mathcal{F}_I(\mathcal{F}_G(\text{HHE}_1(\mathbf{x}))) \quad (3)$$

$$\mathcal{F}_S := \mathcal{F}_S(\text{HHE}_2(\mathbf{x})), \quad (4)$$

where  $\text{HHE}_1, \text{HHE}_2$  denote two sets of hybrid hash encoding,  $\mathcal{F}_G$  denotes geometric features, and  $\mathbf{x}$  denotes a 3D point in the scene.

## C. Panoptic Feature Optimization

**Feature rendering.** Given the density field  $\sigma$  from NeRF, we can render features from the feature field  $\mathcal{F}$  along a given ray  $\mathbf{r}$  using the rendering equation [1]:

$$\hat{\mathcal{F}} := R(\mathcal{F}|\mathbf{r}, \sigma) = \sum_{i=1}^N T_i (1 - e^{-\sigma_i \delta_i}) \mathcal{F}(f(\mathbf{x}_i)) \quad (5)$$

$$T_i = e^{-\sum_{j=1}^{i-1} \sigma_j \delta_j}, \quad (6)$$

where  $\hat{\mathcal{F}}$  denotes rendered features,  $T_i$  denotes the transmittance along ray  $\mathbf{r}$  to sample points  $\mathbf{x}_i$ ,  $\delta_i$  denotes the distance between samples, and  $f(\mathbf{x}_i)$  denotes any function of sample points  $\mathbf{x}_i$ .

**Semantic feature fusion.** Similar to [2], [3], we ground VL embeddings into 3D semantic feature field and derive rendered semantic feature  $\hat{\mathcal{F}}_S$  from geometry features  $\mathcal{F}_G$ . A  $l_1$  loss is applied to optimize the semantic feature field, as shown in Fig. 3(a):

$$\mathcal{L}_S = \left\| \hat{\mathcal{F}}_S - \bar{\mathcal{F}}_S \right\|_1 / C, \quad (7)$$

where  $\hat{\mathcal{F}}_S$  is the rendered semantic features,  $\bar{\mathcal{F}}_S$  is the pre-computed VL embeddings, and  $C$  is the feature dimension.

**Contrastive learning of instance features.** From the instance feature field, we can predict  $\hat{\mathcal{F}}_{\mathcal{I}}$  of every pixel for each viewpoint. With the precomputed instance masks, we apply contrastive learning [37], [38] on the rendered instance features to encourage features on the same instance to be close in the feature space, while being far away across instances. Specifically, to reduce the effect of the high variance during training, we adopt a variant of PointInfoNCE [38] and optimize one positive pair for each backpropagation step. Moreover, we follow the guiding strategy used in [37] by detaching the gradients of reference pixels to further reduce the training variance. Therefore, our contrastive loss  $\mathcal{L}_C$  reads as:

$$\mathcal{L}_C = -\frac{1}{|\Omega^+|} \sum_{(a,p) \in \Omega^+} \log \frac{\exp\left(\hat{\mathcal{F}}_{\mathcal{I}a} \cdot \hat{\mathcal{F}}_{\mathcal{I}p}^d / \tau\right)}{\sum_{(a,n) \in \Omega^-} \exp\left(\hat{\mathcal{F}}_{\mathcal{I}a} \cdot \hat{\mathcal{F}}_{\mathcal{I}n}^d / \tau\right)}, \quad (8)$$

where  $\Omega^+$  and  $\Omega^-$  denote the index set of sampled positive and negative pairs.  $a, p, n$  denote anchor, positive, negative pixels respectively,  $d$  denotes the gradient detaching operation, and  $\tau$  denotes a *temperature* parameter.

It is worth mentioning that the contrastive loss is applied on the rendered viewpoints. As a consequence, despite the absence of any form of association (*e.g.* in the form of instance IDs) between masks that correspond to the same instance in different frames, the underlying reconstructed geometry of PVLFF naturally encourages the features of an instance in different viewpoints to have high similarity upon convergence.

Additionally, inspired by the concentration loss introduced in [20], we adopt a “slow-center” strategy. In particular, after the first training epoch, we estimate the average feature of every instance mask by querying the instance feature field. In the subsequent training epochs, we recompute the average feature and perform an exponential moving average (EMA) update, penalizing through an additional  $l_1$  loss deviations between every anchor feature and its corresponding “slow-center”:

$$\mathcal{L}_{SC} = \frac{1}{|\Omega^+|} \sum_{a \in \Omega^+} \left\| \hat{\mathcal{F}}_{\mathcal{I}a} - \frac{1}{|\mathcal{M}_a|} \sum_{q \in \mathcal{M}_a} \hat{\mathcal{F}}_{\mathcal{I}q}^* \right\|_1, \quad (9)$$

where  $\mathcal{M}_a$  denotes the instance mask from which  $a$  is sampled, and  $\hat{\mathcal{F}}_{\mathcal{I}}^*$  denotes the instance feature field with EMA parameters.

### D. Inference

For instance segmentation, we use a clustering algorithm to directly segment instance features. In our experiments, we use HDBSCAN [39]. For semantic segmentation, we first generate the text embeddings for prompted labels using the text encoder  $E_t^{\text{VL}}$  of the VL model, then compute the similarity between the text embeddings of individual classes and the predicted

semantic features, and assign each predicted feature to the class with the highest similarity score. To further improve this initial segmentation, we fuse the instance information with the semantic information by denoising the semantics inside an instance segment using majority voting. Our method predicts both denoised semantic segmentation and a panoptic segmentation.

## IV. EXPERIMENTS

### A. Experimental Setup

For the open-vocabulary semantic features, we use LSeg [30] to generate dense pixel-level features, and therefore set the feature dimension of  $\mathcal{F}_S$  to 512, the same value as LSeg. For the instance segmenter, we experiment with SAM [35], and set the feature dimension of  $\mathcal{F}_{\mathcal{I}}$  to 8. Both feature fields are modeled by a 3-layer MLP.

### B. Scene-Level Panoptic Segmentation

To the best of our knowledge, there is no previous method capable of open-vocabulary panoptic segmentation. Thus, we compare our method with previous closed-set panoptic segmentation methods in 3D to demonstrate the effectiveness of our system.

**Data.** We present our evaluation results on three public datasets for 3D scenes: Replica [7], ScanNet [8], and HyperSim [6]. Following the same setting as [5], we remap 21 COCO [42] panoptic classes (9 thing + 12 stuff) into the same class set of all datasets for evaluation. To fit a scene, we use RGB and depth images and corresponding poses to optimize PVLFF, while the ground-truth semantic and instance labels are only used for evaluation.

**Metrics.** Panoptic Quality (PQ) is an interpretable and unified metric introduced by [9] to evaluate panoptic segmentation on the image level. To account for the consistency of segmentation across different views in a scene, [5] proposed a modified metric, Scene-level Panoptic Quality ( $\text{PQ}^{\text{scene}}$ ), by merging segments that belong to the same instance or stuff identifier for a certain scene, and computing PQ on the merged segmentation as the evaluation metric. In our experiments, we report  $\text{PQ}^{\text{scene}}$  of our model on the benchmarks to demonstrate the quality of panoptic segmentation. We additionally report the mean Intersection over Union (mIoU) of semantic segmentation to show that our model, which is designed for open-vocabulary queries, has performance comparable to panoptic systems that are trained on a closed set.

**Results.** We compare our model against the state-of-the-art 3D panoptic systems: DM-NeRF [40], Panoptic Neural Fields (PNF) [19], and Panoptic Lifting [5]. Tab. I shows the evaluation results of our model and the baselines. Although designed for open-vocabulary queries, our method achieves semantic segmentation performance comparable to supervised closed-set baselines. On Replica and HyperSim, semantic segmentation of PVLFF improves after denoising with instance prediction. However, on ScanNet we noticed a drop in performance after denoising. We hypothesize that this drop is caused by the poor geometry reconstructed on ScanNet. In particular,

TABLE I

QUANTITATIVE EVALUATION OF PANOPTIC SYSTEMS. WE COMPARE OUR METHOD, WHICH IS DESIGNED FOR *open-vocabulary* QUERIES, AGAINST STATE-OF-THE-ART *close-set* PANOPTIC SYSTEMS ON 8 REPLICA, 12 SCANNET AND 6 HYPERSIM SCENES. OUR METHOD ACHIEVES COMPARABLE PERFORMANCE IN TERMS OF  $PQ^{\text{scene}}$  AND mIoU. WE REPORT THE DENOISED SEMANTIC SEGMENTATION RESULTS OF OUR METHOD IN PARENTHESES.

Method	Replica [7]		ScanNet [8]		HyperSim [6]	
	$PQ^{\text{scene}}$	mIoU	$PQ^{\text{scene}}$	mIoU	$PQ^{\text{scene}}$	mIoU
<i>close-set</i>						
DM-NeRF [40]	44.1	56.0	41.7	49.5	51.6	57.6
PNF [19]	41.1	51.5	48.3	53.9	44.8	50.3
PNF + GT Bounding Boxes	52.5	54.8	54.3	58.7	47.6	58.7
Panoptic Lifting [5]	<b>57.9</b>	<b>67.2</b>	<b>58.9</b>	65.2	<b>60.1</b>	<b>67.8</b>
<i>open-vocabulary</i>						
Ours – PVLFF	43.5	57.5 (59.4)	44.0	<b>67.1</b> (60.8)	39.4	50.0 (52.9)

TABLE II

SEMANTIC SEGMENTATION OF ZERO-SHOT SYSTEMS. WE EVALUATE OUR METHOD AND COMPARE AGAINST THE BASELINES ON 312 SCANNET SCENES. OUR METHOD OUTPERFORMS OTHER ZERO-SHOT SEMANTIC SYSTEMS ON mIoU IN BOTH 3D AND 2D SEGMENTATION TASKS, WHILE ACHIEVING COMPARABLE mAcc. WE REPORT THE DENOISED SEMANTIC SEGMENTATION RESULTS OF OUR METHOD IN PARENTHESES.

Method	ScanNet [8]	
	mIoU	mAcc
OpenScene [32] - LSeg (3D)	54.2	66.6
OpenScene - OpenSeg (3D)	47.5	<b>70.7</b>
NIVLFF [3] (3D)	47.4	55.8
Ours – PVLFF (3D)	<b>58.8</b> (47.5)	70.2 (59.3)
MSeg [41] (2D)	45.6	54.4
NIVLFF (2D)	62.5	<b>80.2</b>
Ours – PVLFF (2D)	<b>67.4</b> (58.9)	75.7 (66.6)

as can be noted in Fig. 4, instance and semantic features are more blurred on ScanNet than Replica and HyperSim. In terms of  $PQ^{\text{scene}}$ , our system produces lower scores. The reason for this is that unlike the closed-set systems, which are trained on the specific classes evaluated, our method relies on the universal segmenter SAM to precompute instance masks; due to its object-agnostic nature, SAM is subject to over-segmentation. We note however that defining the boundaries of a previously unseen instance is inherently an ill-posed problem. Consider for example the ceiling in the picture in the first row of Fig. 4: Without previously defining whether each tile should be considered as a part of a single “ceiling” instance or rather as a separate instance, it is not possible to guarantee that the detected boundaries will reflect those defined used in the ground-truth data. An important observation, however, is that despite the inherent ambiguity of the problem, as we show in Sec. IV-D PVLFF predicts continuous instance features which are hierarchically structured. This hierarchy could potentially be used to produce panoptic segmentations of different granularities.

### C. Open-Vocabulary Semantic Segmentation

To demonstrate the power of the open-vocabulary capabilities of PVLFF, we further compare our model against current zero-shot systems, namely MSeg [41], OpenScene [32] (LSeg [30] / OpenSeg [31]), and NIVLFF [3]. We evaluate quantitatively on the 3D semantic segmentation benchmark of ScanNet [8], computing mIoU and mean Accuracy (mAcc) of

20 ScanNet classes in the validation set for 3D and 2D segmentation respectively. For neural-field methods like NIVLFF and ours, we compute the 3D point cloud segmentation by querying the semantic feature for each point and then assigning semantics according to the similarities with the label text embeddings, and we compute the 2D image segmentation by similarly segmenting rendered semantic feature maps for each viewpoint of every scene scan.

**Evaluation on ScanNet.** We compare the performance of our model against baselines in pointcloud segmentation and image segmentation on the ScanNet [8] validation set. For point cloud segmentation (3D), we predict semantic labels for each ground-truth point on the scene level. For image segmentation (2D), we predict image semantic segmentation for each viewpoint of every scene. Note that OpenScene is given the advantage of using ground-truth 3D point cloud, while NeRF-based methods, like NIVLFF and ours, reconstruct the scene geometry implicitly from 2D posed images. As shown in Tab. II, our model outperforms state-of-the-art methods in point cloud segmentation. In terms of image segmentation on rendered images, PVLFF produces comparable results of semantic understanding, while PVLFF is also capable of segmenting instances.

**Qualitative Visual Results.** In Fig. 4 we present the visual results of PVLFF on different datasets with language prompts of 101 Replica [7] classes. The instance feature field can segment scenes into multiple instances with good quality, and can even segment based on textures. For example, in scene0616\_00, PVLFF segments wall into different parts based on the paintings on the wall. For semantic segmentation, PVLFF can predict rare categories correctly that are not recognized by the closed-set panoptic systems (Sec. IV-B), such as laptop, mat, monitor, etc. However, the visual encoder of LSeg [30] is trained on ADE20K [43], a small closed-set dataset. Therefore, PVLFF inherently performs worse in certain categories, such as lamp and door. In this sense, LSeg becomes the bottleneck of our system, which we would like to address in future work.

### D. Hierarchical Instance Features

Since we use SAM [35] as instance segmenter in our pre-processing step, we are not using instance masks of a certain

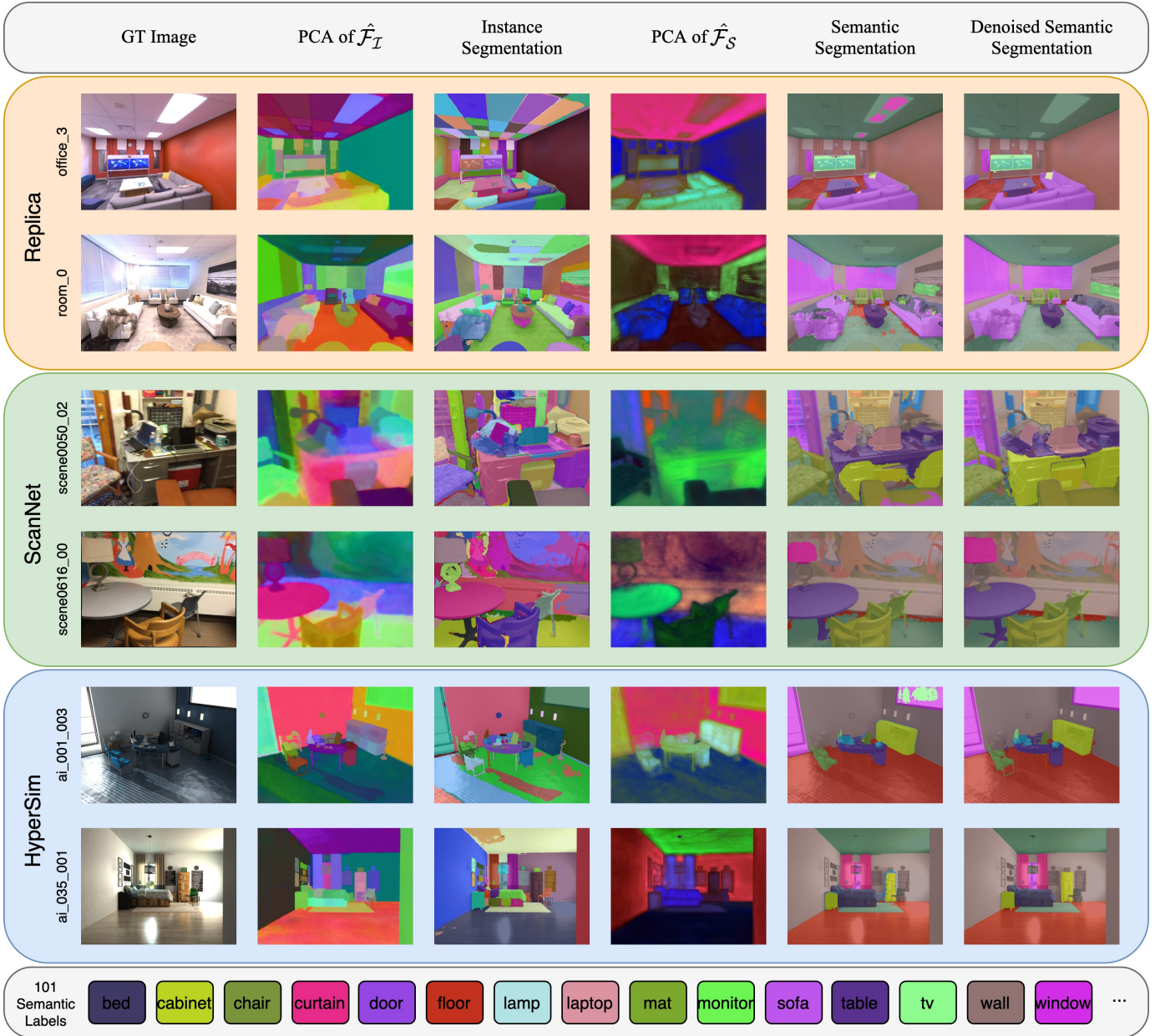


Fig. 4. **PVLFF with Open-Vocabulary language queries.** We query PVLFF with 101 Replica [7] semantic prompts, and visualize the instance and semantic features through PCA. We show the instance segmentation results directly from HDBSCAN [39] and the semantic segmentation together the denoised one.

training set, but building the scene representation upon the general masks, which can be masks of multi-level parts of an instance. Therefore, our instance feature field is hierarchically constructed by contrastive learning, enabling different levels of instance segmentation.

In Fig. 5, we show the hierarchical instance features of PVLFF and visualize different levels of instance predictions for sofa and ceiling. With such hierarchical instance features, PVLFF provides the possibility to perform zero-shot panoptic segmentation on different granularities. Note that we use predictions at the finest level of clustering for the evaluations above. Potentially, an adaptive strategy for certain categories (*e.g.*, sofa, bed, *etc.*), which determines the best

level of instance segmentation from the hierarchical clustering tree, would improve the evaluation results.

### E. Ablation

In Tab. III, we show an ablation of different model designs by evaluating instance and semantic segmentation on HyperSim [6]. We investigate the influence of different design settings on the model performance, and report how different semantic features affect instance segmentation. For instance segmentation, we measure mean (weighted) coverage (mCov, mWCov) [44] to evaluate the instance-wise IoU of prediction for every ground-truth. For semantic segmentation, we measure mIoU and mAcc of both direct prediction from semantic field and denoised prediction.

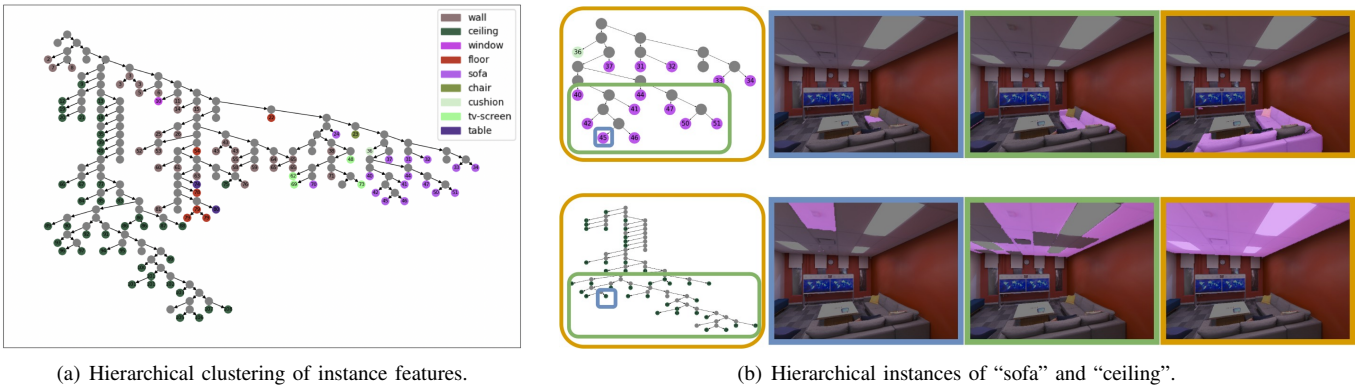


Fig. 5. **Hierarchical instance features of PVLFF.** We run HDBSCAN on predicted instance features of a Replica scene and visualize the clustering results. In the clustering tree, each node with color represents a predicted instance and the number inside the node represents its instance ID. PVLFF, by default, over-segments an instance, since we use SAM for precomputed instance masks, which is a universal segmenter and produces multi-levels of segmentation without any constrains of certain instance types. Thus, PVLFF inheritably predicts segments agnostically. However, by building the clustering tree, we can recover different levels of instance predictions. We show the hierarchical predictions of “sofa” and “ceiling” by visualizing corresponding sub-structures in the clustering tree.

TABLE III

ABLATION OF DESIGN CHOICES ON HYPERSIM. WE REPORT THE INFLUENCE OF OUR MODEL DESIGN CHOICES ON INSTANCE (mCov, mWCov) AND SEMANTIC (mIoU, mAcc) QUALITIES, AND ABULATE THE EFFECT OF DIFFERENT SEMANTIC FEATURES. THE DENOISED SEMANTIC SEGMENTATION RESULTS ARE PRESENTED IN THE PARENTHESES.

Feature HHE <sup>1</sup>	Feature Decoupling <sup>2</sup>	Instance Feature	Semantic Feature	mCov	mWCov	mIoU (mIoU*)	mAcc (mAcc*)
X	X	X	LSeg	-	-	47.7	58.7
X	X	✓	LSeg	56.6	48.4	50.9 (49.5)	62.3 (58.9)
✓	X	✓	LSeg	64.8	52.3	50.6 (51.3)	62.2 (60.8)
✓	X	✓	X	66.8	52.9	-	-
✓	X	✓	DINO	65.0	52.1	-	-
✓	✓	✓	LSeg	<b>68.3</b>	<b>54.1</b>	50.0 ( <b>52.9</b> )	61.0 ( <b>63.0</b> )

<sup>1</sup> “Feature HHE” denotes using another HHE for the underlying feature representation.

<sup>2</sup> “Feature Decoupling” denotes separating semantic and instance feature fields into two branches.

As a baseline [3] (row 1 in Tab. III), we evaluate the model that stacks a VL feature head on the scene reconstruction branch. We find that introducing instance feature (row 2) improves the semantic performance compared to the baseline. We further show that by optimizing features on a different HHE branch (row 3), the model can largely increase the instance segmentation quality, while achieving similar semantic results. We also investigate the influence of different semantic features (row 4, 5) on the quality of instance features. Without storing any semantic information, the model (row 4) can fully use feature HHE for instance features, while models with semantic features (row 3, 5) have slightly worse but still comparable instance segmentation qualities. Note that the evaluations are under open-vocabulary queries. Thus, the model with DINO (row 5) doesn’t predict semantic segmentation. Finally, we show that our method (last row) with the feature decoupling strategy can greatly improve the instance features, and produces the best denoised semantic segmentation after fusing instance prediction.

## V. CONCLUSION AND FUTURE WORK

In this paper, we propose PVLFF, a system for open-vocabulary panoptic segmentation that reconstructs a scene implicitly as a neural radiance field, while simultaneously op-

timizing panoptic feature fields for scene understanding in an open-set. We distill off-the-shelf vision-language embeddings into a semantic feature field, and train an instance feature field from object-agnostic 2D proposals through contrastive learning. We showed that decoupling the features into two branches enhances the robustness and capacity of the neural scene representation. We validated our model design and evaluated against state-of-the-art semantic and panoptic segmentation methods on different datasets.

A part which was only partly studied in this work is the *query-dependency* of the instance segmentation in open-vocabulary panoptic segmentation systems. For example, when asking the system to segment individual keys of a keyboard vs. the entire keyboard, the correct segmentation would be different. In our system, the instance segments are learned directly from object-agnostic 2D proposals, which do not take into account the query. As a consequence, we inherit the object instance bias in those initial 2D segmentation proposals. Future work might focus on making the clustering step dependent on the query or otherwise producing a panoptic segmentation which takes into account the query.

## REFERENCES

- [1] B. Mildenhall, P. P. Srinivasan, M. Tancik, J. T. Barron, R. Ramamoorthi, and R. Ng, “Nerf: Representing scenes as neural radiance fields for view

- synthesis,” in *Eur. Conf. Comput. Vis.*, 2020.
- [2] J. Kerr, C. M. Kim, K. Goldberg, A. Kanazawa, and M. Tancik, “Lerf: Language embedded radiance fields,” *arXiv:2303.09553*, 2023.
  - [3] K. Blomqvist, F. Milano, J. J. Chung, L. Ott, and R. Siegwart, “Neural implicit vision-language feature fields,” *arXiv:2303.10962*, 2023.
  - [4] K. Liu, F. Zhan, J. Zhang, M. Xu, Y. Yu, A. E. Saddik, C. Theobalt, E. Xing, and S. Lu, “3d open-vocabulary segmentation with foundation models,” *arXiv:2305.14093*, 2023.
  - [5] Y. Siddiqui, L. Porzi, S. R. Bulò, N. Müller, M. Nießner, A. Dai, and P. Kotschieder, “Panoptic lifting for 3d scene understanding with neural fields,” in *IEEE Conf. Comput. Vis. Pattern Recog.*, 2023, pp. 9043–9052.
  - [6] M. Roberts, J. Ramapuram, A. Ranjan, A. Kumar, M. A. Bautista, N. Paczan, R. Webb, and J. M. Susskind, “Hypersim: A photorealistic synthetic dataset for holistic indoor scene understanding,” in *Int. Conf. Comput. Vis.*, 2021.
  - [7] J. Straub, T. Whelan, L. Ma, Y. Chen, E. Wijmans, S. Green, J. J. Engel, R. Mur-Artal, C. Ren, S. Verma, A. Clarkson, M. Yan, B. Budge, Y. Yan, X. Pan, J. Yon, Y. Zou, K. Leon, N. Carter, J. Briales, T. Gillingham, E. Mueggler, L. Pesqueira, M. Savva, D. Batra, H. M. Strasdat, R. D. Nardi, M. Goesele, S. Lovegrove, and R. Newcombe, “The Replica dataset: A digital replica of indoor spaces,” *arXiv:1906.05797*, 2019.
  - [8] A. Dai, A. X. Chang, M. Savva, M. Halber, T. Funkhouser, and M. Nießner, “ScanNet: Richly-annotated 3d reconstructions of indoor scenes,” in *IEEE Conf. Comput. Vis. Pattern Recog.*, 2017, pp. 5828–5839.
  - [9] A. Kirillov, K. He, R. Girshick, C. Rother, and P. Dollár, “Panoptic segmentation,” in *IEEE Conf. Comput. Vis. Pattern Recog.*, 2019, pp. 9396–9405.
  - [10] B. Cheng, I. Misra, A. G. Schwing, A. Kirillov, and R. Girdhar, “Masked-attention mask transformer for universal image segmentation,” in *IEEE Conf. Comput. Vis. Pattern Recog.*, 2022, pp. 1290–1299.
  - [11] B. Cheng, M. D. Collins, Y. Zhu, T. Liu, T. S. Huang, H. Adam, and L.-C. Chen, “Panoptic-deeplab: A simple, strong, and fast baseline for bottom-up panoptic segmentation,” in *IEEE Conf. Comput. Vis. Pattern Recog.*, 2020, pp. 12475–12485.
  - [12] W. K. Fong, R. Mohan, J. V. Hurtado, L. Zhou, H. Caesar, O. Beijbom, and A. Valada, “Panoptic nusenes: A large-scale benchmark for lidar panoptic segmentation and tracking,” *IEEE Robot. Automat. Letters*, vol. 7, no. 2, pp. 3795–3802, 2022.
  - [13] K. Sirohi, R. Mohan, D. Büscher, W. Burgard, and A. Valada, “Efficientlps: Efficient lidar panoptic segmentation,” *IEEE Trans. Robot.*, vol. 38, no. 3, pp. 1894–1914, 2021.
  - [14] J. Schult, F. Engelmann, A. Hermans, O. Litany, S. Tang, and B. Leibe, “Mask3d for 3d semantic instance segmentation,” *arXiv:2210.03105*, 2022.
  - [15] M. Grinvald, F. Furrer, T. Novkovic, J. J. Chung, C. Cadena, R. Siegwart, and J. Nieto, “Volumetric Instance-Aware Semantic Mapping and 3D Object Discovery,” *IEEE Robot. Automat. Letters*, vol. 4, no. 3, pp. 3037–3044, July 2019.
  - [16] M. Dahnert, J. Hou, M. Nießner, and A. Dai, “Panoptic 3d scene reconstruction from a single rgb image,” *Adv. Neural Inform. Process. Syst.*, vol. 34, pp. 8282–8293, 2021.
  - [17] G. Narita, T. Seno, T. Ishikawa, and Y. Kaji, “Panopticfusion: Online volumetric semantic mapping at the level of stuff and things,” in *IEEE Int. Conf. Intell. Robot. Syst.* IEEE, 2019, pp. 4205–4212.
  - [18] X. Fu, S. Zhang, T. Chen, Y. Lu, L. Zhu, X. Zhou, A. Geiger, and Y. Liao, “Panoptic nerf: 3d-to-2d label transfer for panoptic urban scene segmentation,” in *Int. Conf. 3D Vis.*, 2022.
  - [19] A. Kundu, K. Genova, X. Yin, A. Fathi, C. Pantofaru, L. Guibas, A. Tagliasacchi, F. Dellaert, and T. Funkhouser, “Panoptic Neural Fields: A Semantic Object-Aware Neural Scene Representation,” in *IEEE Conf. Comput. Vis. Pattern Recog.*, 2022.
  - [20] Y. Bhalgat, I. Laina, J. F. Henriques, A. Zisserman, and A. Vedaldi, “Contrastive lift: 3d object instance segmentation by slow-fast contrastive fusion,” *arXiv:2306.04633*, 2023.
  - [21] K. Deng, A. Liu, J.-Y. Zhu, and D. Ramanan, “Depth-supervised nerf: Fewer views and faster training for free,” in *IEEE Conf. Comput. Vis. Pattern Recog.*, 2022, pp. 12882–12891.
  - [22] J. T. Barron, B. Mildenhall, M. Tancik, P. Hedman, R. Martin-Brualla, and P. P. Srinivasan, “Mip-nerf: A multiscale representation for anti-aliasing neural radiance fields,” in *IEEE Conf. Comput. Vis. Pattern Recog.*, 2021, pp. 5855–5864.
  - [23] A. Chen, Z. Xu, A. Geiger, J. Yu, and H. Su, “Tensorf: Tensorial radiance fields,” in *Eur. Conf. Comput. Vis.* Springer, 2022, pp. 333–350.
  - [24] S. Zhi, T. Laidlow, S. Leutenegger, and A. Davison, “In-place scene labelling and understanding with implicit scene representation,” in *Int. Conf. Comput. Vis.*, 2021.
  - [25] V. Tschernezki, I. Laina, D. Larlus, and A. Vedaldi, “Neural feature fusion fields: 3d distillation of self-supervised 2d image representations,” in *Int. Conf. 3D Vis.* IEEE, 2022, pp. 443–453.
  - [26] A. Radford, J. W. Kim, C. Hallacy, A. Ramesh, G. Goh, S. Agarwal, G. Sastry, A. Askell, P. Mishkin, J. Clark *et al.*, “Learning transferable visual models from natural language supervision,” in *Int. Conf. Mach. Learn.* PMLR, 2021, pp. 8748–8763.
  - [27] M. Xu, Z. Zhang, F. Wei, H. Hu, and X. Bai, “Side adapter network for open-vocabulary semantic segmentation,” in *IEEE Conf. Comput. Vis. Pattern Recog.*, 2023, pp. 2945–2954.
  - [28] M. Yi, Q. Cui, H. Wu, C. Yang, O. Yoshie, and H. Lu, “A simple framework for text-supervised semantic segmentation,” in *IEEE Conf. Comput. Vis. Pattern Recog.*, 2023, pp. 7071–7080.
  - [29] F. Liang, B. Wu, X. Dai, K. Li, Y. Zhao, H. Zhang, P. Zhang, P. Vajda, and D. Marculescu, “Open-vocabulary semantic segmentation with mask-adapted clip,” in *IEEE Conf. Comput. Vis. Pattern Recog.*, 2023, pp. 7061–7070.
  - [30] B. Li, K. Q. Weinberger, S. Belongie, V. Koltun, and R. Ranftl, “Language-driven semantic segmentation,” in *Int. Conf. Learn. Represent.*, 2022.
  - [31] G. Ghiasi, X. Gu, Y. Cui, and T.-Y. Lin, “Scaling open-vocabulary image segmentation with image-level labels,” in *Eur. Conf. Comput. Vis.* Springer, 2022, pp. 540–557.
  - [32] S. Peng, K. Genova, C. Jiang, A. Tagliasacchi, M. Pollefeys, T. Funkhouser *et al.*, “Openscene: 3d scene understanding with open vocabularies,” in *IEEE Conf. Comput. Vis. Pattern Recog.*, 2023, pp. 815–824.
  - [33] Z. Liu, X. Qi, and C.-W. Fu, “3d-to-2d distillation for indoor scene parsing,” in *IEEE Conf. Comput. Vis. Pattern Recog.*, 2021, pp. 4464–4474.
  - [34] M. Ahn, A. Brohan, N. Brown, Y. Chebotar, O. Cortes, B. David, C. Finn, C. Fu, K. Gopalakrishnan, K. Hausman *et al.*, “Do as i can, not as i say: Grounding language in robotic affordances,” *arXiv:2204.01691*, 2022.
  - [35] A. Kirillov, E. Mintun, N. Ravi, H. Mao, C. Rolland, L. Gustafson, T. Xiao, S. Whitehead, A. C. Berg, W.-Y. Lo, P. Dollár, and R. Girshick, “Segment anything,” *arXiv:2304.02643*, 2023.
  - [36] K. Blomqvist, L. Ott, J. J. Chung, and R. Siegwart, “Baking in the feature: Accelerating volumetric segmentation by rendering feature maps,” *arXiv:2209.12744*, 2022.
  - [37] L. Jiang, S. Shi, Z. Tian, X. Lai, S. Liu, C.-W. Fu, and J. Jia, “Guided point contrastive learning for semi-supervised point cloud semantic segmentation,” in *IEEE Conf. Comput. Vis. Pattern Recog.*, 2021, pp. 6423–6432.
  - [38] S. Xie, J. Gu, D. Guo, C. R. Qi, L. Guibas, and O. Litany, “Pointcontrast: Unsupervised pre-training for 3d point cloud understanding,” in *Eur. Conf. Comput. Vis.* Springer, 2020, pp. 574–591.
  - [39] L. McInnes, J. Healy, and S. Astels, “hdbscan: Hierarchical density based clustering,” *J. Open Source Software*, vol. 2, no. 11, p. 205, 2017.
  - [40] W. Bing, L. Chen, and B. Yang, “Dm-nerf: 3d scene geometry decomposition and manipulation from 2d images,” *arXiv:2208.07227*, 2022.
  - [41] J. Lambert, Z. Liu, O. Sener, J. Hays, and V. Koltun, “MSeg: A composite dataset for multi-domain semantic segmentation,” in *IEEE Conf. Comput. Vis. Pattern Recog.*, 2020.
  - [42] T.-Y. Lin, M. Maire, S. Belongie, J. Hays, P. Perona, D. Ramanan, P. Dollár, and C. L. Zitnick, “Microsoft coco: Common objects in context,” in *Eur. Conf. Comput. Vis.* Springer, 2014, pp. 740–755.
  - [43] B. Zhou, H. Zhao, X. Puig, S. Fidler, A. Barriuso, and A. Torralba, “Scene parsing through ade20k dataset,” in *IEEE Conf. Comput. Vis. Pattern Recog.*, 2017, pp. 633–641.
  - [44] X. Wang, S. Liu, X. Shen, C. Shen, and J. Jia, “Associatively segmenting instances and semantics in point clouds,” in *IEEE Conf. Comput. Vis. Pattern Recog.*, 2019, pp. 4096–4105.